A Performance-Driven Approach for the Design of Cellular Geometries with Low Thermal Conductivity for Application in 3D-Printed Façade Components

Piccioni, Valeria; Turrin, Michela; Tenpierik, Martin

Publication date
2020

Document Version
Final published version

Published in
Proceedings of the Symposium on Simulation for Architecture and Urban Design (SimAUD 2020)

SYMPOSIUM ON SIMULATION IN ARCHITECTURE + URBAN DESIGN
SimAUD 2020

A Performance-Driven Approach for the Design of Cellular Geometries with Low Thermal Conductivity for Application in 3D-Printed Façade Components

Valeria Piccioni[1], Michela Turrin[2] and Martin J. Tenpierik[2]

[1]Delft University of Technology
Delft, Netherlands
valeria1.piccioni@gmail.com

[2]Delft University of Technology
Delft, Netherlands
{m.turrin, m.j.tenpierik}@tudelft.nl

ABSTRACT

Additive manufacturing allows the fabrication of complex geometries with enhanced performances, making it interesting for application in façade components. Assessing the performance of non-standard geometries and 3D printed parts requires a combination of digital and analytical methods to retrieve validated models which can guide the design process. In this study a 3D printed mono-material façade component was designed, where the complex geometrical configuration enhance its thermal insulation properties. For this, a digital workflow was developed, encompassing performance-driven design, performance assessment and geometry generation for fabrication.

Analytical heat transfer models, heat flux measurements, and heat transfer simulations with COMSOL Multiphysics were used to assess the thermal properties of different geometrical alternatives. By observing and comparing the results, a validated model was defined to retrieve design guidelines and thermal performance indicators. The results identify porosity as the driving factor for thermal insulation and clarify the nature of the heat transfer in 3D printed cellular structures. Open surface-based geometries were preferred for the good combination of thermal properties and manufacturability. The findings are embedded in a digital workflow in Rhino-Grasshopper, enabling the design of insulating cellular structures to be used in 3D printed façade components.

Author Keywords

Thermal insulation; FEA simulations; Parametric Design; Additive Manufacturing; Façade design; Performance-driven design

ACM Classification Keywords

Applied computing – Arts and Humanities – Architecture (buildings) – Computer-Aided Design

1. INTRODUCTION

Additive manufacturing (AM) is currently being investigated for application in the building industry, suggesting a revolution in the way products are designed, manufactured and distributed to the end users (Gao et al. 2015). The versatile form of fabrication enhances the possibility of integrating performance-driven features in the design, without having to compromise on optimality due to manufacturing limitations. In this prospective, the use of digital tools and simulations is needed to deal with the increased complexity of non-standard components. When compared to traditional manufacturing techniques, AM shows some unique capabilities that suggest a potential application for the built environment. Geometrical complexity can be easily achieved so that optimised and customised shapes are possible. Material complexity is also made possible by manipulating geometry at meso-scale so that materials can be designed to obtain different properties where needed, as presented by Ashby (2006).

The building envelope is in itself one of the most complex parts of the building. Recently, the challenging objectives for energy performance set by new regulations, such as the European EPBD, have redefined the role of façades in the overall building concept, with stringent requirements in terms of materials and performance, especially thermal control. From the scientific community and industries, existing research on AM for the building envelope has proved to be promising for the design of multi-functional façade components with complex geometries for climate control, as presented by Sarakinioti et al. (2018). Among the key requirements of the building envelope, thermal performance is a most promising aspect to be investigated as it can be controlled by the geometry of the component and contribute to savings in terms of material and energy consumption. In particular, thermal insulation is a property which is strongly related to the geometry of the problem and different thermal conductivity values can be achieved with the same material by changing its meso-structure as presented by Gooskens (2016).

This study proposes a novel digital workflow, based on the results of FE simulations, analytical models and physical testing, to design thermally insulating cellular structures and assess their performance. In this context, a research-and-design workflow is proposed integrating digital and physical tools. The workflow is used to design a mono-material façade panel to be additively manufactured, which serves as a filter between the interior and exterior environment. The chosen fabrication method is Fused Deposition Modelling which is a relatively low-cost and

accessible AM technique based on material extrusion (Wu et al. 2016). Among the materials suitable for this technique, polymers were chosen for their low thermal conductivity and the possibility of being printed at different resolutions (Ngo et al. 2018).

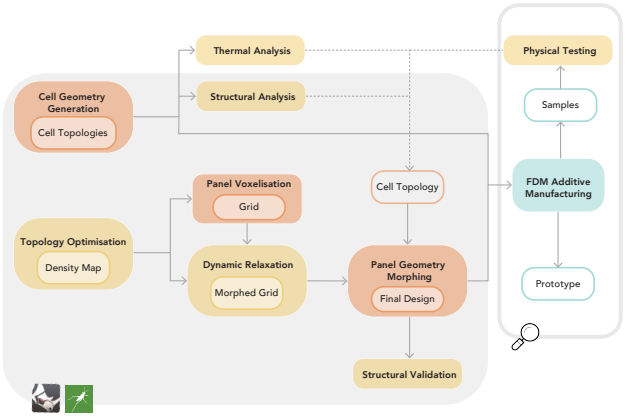

Figure 1: Digital and physical workflow defined for the study, consisting of parametric modelling in the environment of Rhino+Grasshopper, prototyping and physical testing

2. METHOD

The research focused on identifying a method to assess the thermal performance enhanced by the complex geometrical configurations and integrate it into a digital design workflow. The workflow was used to propose the design of a modular façade component, serving as a filter between the interior and exterior environment. The chosen fabrication method is Fused Deposition Modelling which is a relatively low-cost and accessible AM technique, based on material extrusion (Wu et al. 2016). This has proved to be suitable for the production of large scale architectural components in several realised projects, such as the Canal House designed by Dus Architects in 2013 (3DPrint Canal House n.d.). Among the materials suitable for this technique, polymers were chosen for further exploration for the low thermal conductivity, the possibility of being printed at different resolutions and the suitability for the FDM process (Ngo et al. 2018). Considering recyclability, non-toxicity and its low cost, PETG was identified as the material to investigate, combining good thermal properties and low density.

For this study, a combination of research through design and performance-driven design was adopted as methodology. This involved retrieving performance indicators using analytical, numerical and experimental methods and comparing results to verify the reliability of the proposed methods. According to the guidelines given by the results of the validated models, geometrical alternatives were first generated, then assessed and developed into a façade component. Firstly, background studies were used to define the boundary conditions for the design in terms of component scale, production process, material, morphologies and target performances. Then, different geometrical alternatives were explored and their performance was assessed using analytical models, physical testing and software simulations. The different options were compared and assessed according to their thermal insulation (effective thermal conductivity) and manufacturability with AM techniques. Finally, the chosen cellular geometry was used to design the façade component using topology optimisation principles.

The use of digital tools was essential for the generation of design alternatives and integration of performance-driven guidelines. FE simulations on Comsol Multiphysics were used to study the thermal behaviour in complex geometrical structures which analytical models are not able to describe accurately. To combine these aspects, a digital workflow was defined, in the parametric environment of Rhinoceros 3D and Grasshopper, which includes geometry generation and morphing procedures as well as performance assessment, with a direct connection to the additive manufacturing production process.

3. GEOMETRY EXPLORATION OF CELLULAR STRUCTURES

Geometrical complexity at meso-scale was addressed by studying the properties of cellular solids according to the models proposed by Ashby (2006). On a first categorisation cellular solids can be described as either strut-based geometries, such as lattices, or surface-based geometries, such as foams and shells. Among shells, triply periodic minimal surfaces are known to have interesting thermal insulating properties due to their low surface-to-volume ratio (Maskery et al. 2018). Lattices can be mathematically defined as arrays of points generated by a set of translations in a 3-dimensional space, while shells can be described by an implicit surface equation.

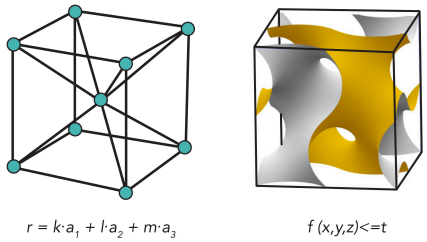

Figure 2: Examples of cellular geometries: lattice and shell

Using their geometrical definition, nine different cell topologies were modelled in the parametric environment of Rhino-Grasshopper and analysed (Figure 3). These typologies were selected according to performance and manufacturability guidelines. In relation to thermal insulation, geometries which take advantage of the low conductivity of enclosed air cavities were chosen along with porous structures which are able to hinder the path of heat transfer. Finally, considering production with additive manufacturing, self-supporting geometries were preferred in order to minimise the use of support material. Moreover, to minimise printing time, topologies which allow for a continuous path of the extruder during printing were selected. According to the findings of Oarakinioti et al. (2018), an elongated cell size was designed with a minimum dimension of 3 cm in the direction of the heat

flow. This was done to minimise convective heat flow within the geometry, while the other dimensions were kept around 15 cm.

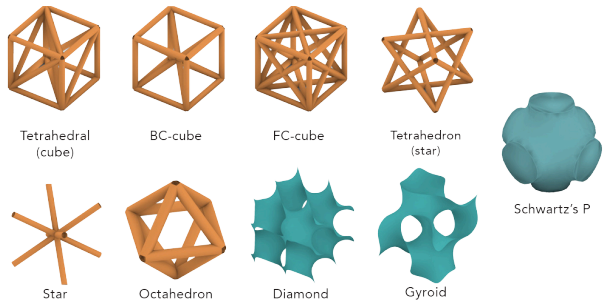

Figure 3: Selected cell topologies for design exploration based on performance and manufacturability parameters

3.1. Analytical Models for Thermal Performance

At first, different analytical models were used to calculate the effective thermal conductivity of cellular structures. These expressions are mainly dependent on the density of the geometry and cannot accurately account for the effect of topology. They were useful to make a preliminary comparison between the different options. The analytical model proposed by Hegman and Babscan (2018) was used to assess the different geometries. This model analyses the problem in terms of two limiting cases, the parallel and series arrangement of the solid and gaseous constituents, and was defined for application to any cellular geometry. It considers only conductive heat transfer mode and was used to retrieve an effective thermal conductivity value. From this model, an effective thermal conductivity for each cell topology was retrieved. The results of the analytical calculations show that thermal performance increases with relative density, with nearly linear relationship (Figure 4). These results are compared with those of simulations and physical tests to assess how geometry influences the two performances in more detail.

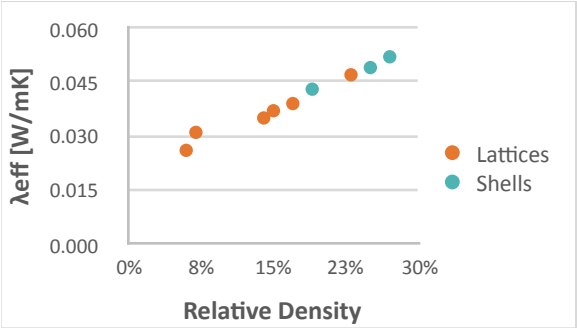

Figure 4: Relation between porosity and thermal insulation

3.2. Physical Testing on 3D-printed Samples

Geometry samples were produced using Fused Deposition Modelling technique with a LeapFrog desktop printer and PETG filament. The size of the samples was defined according to the machine built volume and to the set-up of the heat flux physical test. Geometry samples of 25 x 17 x 1.7 cm were modelled in Grasshopper, corresponding to a 3 x 2 cell array. The chosen cell size is 8.3 x 8.5 x 1.7 cm, with the smallest dimension in the direction of the heat transfer. Shell geometries were found to be particularly suitable for manufacturing with FDM (Figure 5-6). The printing of lattice structures proved to be more challenging due to the horizontal slicing, which results in steep overhanging geometries that require support material. To efficiently produced such geometries power bed fusion techniques could be used or a robotic arm coupled with an extruder for multi-plan printing.

Physical tests were carried out according to the standardised heat flow meter testing procedure (Meng et al. 2015) to retrieve the effective thermal conductivity of the printed samples. Because the surface of the sample was not flat, a VIVAK (PETG) sheets had to be added to make sure the sensors had proper contact and to close off possible air gaps that were present in the geometry sample.

The samples of size 25 x 17 x 1.7 cm were put within a hole in one of the faces of a polystyrene box of 1 m3 volume. Inside the box, a shielded light bulb was switched on, heating up the box until around 46°C and creating a temperature difference with the external environment at room temperature. After thermal equilibrium condition was reached, where net flow of thermal energy between the two systems is constant, steady-state measurements were performed by measuring the surface temperature of both sides of the sample and of the air on both sides with type T thermocouples and by measuring the heat flux on both sides of the sample using two Hukseflux HFP01 heat flux plates. Since the heat flux sensor can only measure a circular area of 32 mm diameter, the measurements were done twice per sample, as in Figure 7: first with the sensor pointed at a solid portion of the sample and then with the sensor pointed at a void part of the sample.

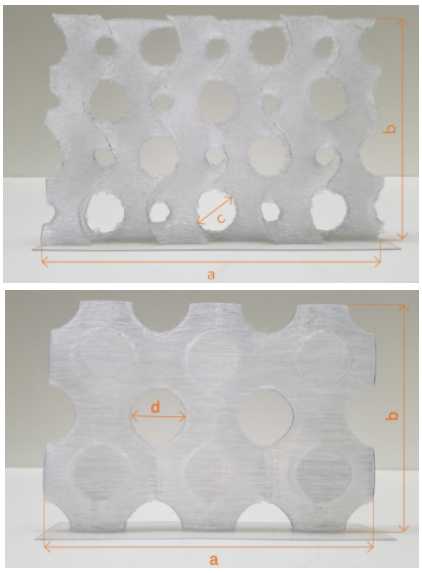

Figure 5- 6: 3D printed samples of Gyroid cell array (top) and Schwartz's P cell array (bottom). Dimensions: a= 25 cm, b=17 c= 4 cm, thickness=1.7 cm

Geometry	Ts_{in} [°C]	Ts_{out} [°C]	Heat Flux (+) [μV]	Heat Flux (-) [μV]	Sensitivity (+) [V/(W/m²)]	Sensitivity (-) [V/(W/m²)]	Q [W/m²]	R_{tot} [m²K/W]	λ_{eff} AV [W/mK]
#1 Diamond	46,4	26,1	3,92	2,98	6 2,23	61,22	55,8	0,364	0,063
#2 Diamond	46,3	28,3	4,58	4,1	62,23	61,22	70,3	0,256	
#1 Gyroid	46,7	28,8	3,64	3,84	62,23	61,22	60,6	0,295	0,071
#2 Gyroid	46,7	28,2	5,58	3,76	62,23	61,22	75,5	0,245	
#1 Schwartz's P	47,8	27,7	3,94	4,04	62,23	61,22	64,7	0,311	0,069
#2 Schwartz's P	50,8	28,9	5,82	5,14	62,23	61,22	88,7	0,247	

Figure 7: Results of heat transfer tests on 3D printed samples

The measurement instruments were connected to a data logging system (Eltek Squirrel 1000 series), transferring the data to the Darca Software. From these heat flux and temperature data (Figure 7), the thermal resistance and thereby also the effective thermal conductivity was calculated according to the following relation:

$$\lambda_{eff} = \frac{d \bullet q}{(T_{s1} - T_{s2})}$$

where T_{s1} and T_{s2} are the temperatures measured at the sample's exterior sides, d is the thickness of the sample and q is the measured heat flow.

According to the results (Figure 7), the three geometries exhibit similar thermal conductivity in the range of 0.07 W/(m·K), which corresponds to a decrease of 65% compared to the thermal conductivity of the solid PETG (λ=0,19 W/(m·K)).

3.3. Software Simulations for Thermal Performance

As a next step, FE simulations were performed using Comsol Multiphysics version 5.4 to gain insight into the thermal behaviour of the different geometries, with three main objectives: compare and verify the results from the physical tests, define a reliable model to test the thermal conductivity of different geometries and retrieve the effective thermal conductivity of lattice geometries that could not be tested. The simulations were performed in different steps, in order to evaluate the relations between geometry and the different heat transfer modes first separately and then combined. Moreover, varying parameters such as cell size, cell topology and cell array were introduced to find the best geometrical combination (Figure 8).

FE modelling of heat transfer through cellular structures proved to be expensive from a computational point of view, due to the complexity of the geometries involved, particularly for shell geometries. The final simulation model took into account conductive heat transfer directly while convection and radiation are accounted for using the simplified methodology of an effective thermal conductivity of air as proposed in NEN-EN-ISO 6946 (Nederlands Normalisatie Instituut, 2008). This model was validated by comparing the results of the simulations with those of the physical tests. For the simulations 'the heat transfer in solids' module was used in combination with steady-state simulations. Two convective heat fluxes through non-solid material were defined at the interior and exterior sides of the geometry, specifying the heat transfer coefficients according to common calculation methods: 7.8 W/m²·K for the interior flux and 25 W/m²·K for the exterior. The sides of the panel were assigned an insulation boundary to represent adiabatic conditions and the front and back of the panel were assigned a fixed temperature of 20°C and 0°C respectively. Furthermore, as thermal conductivity of the PETG filament, 0.19 W/(m·K), was used; the effective thermal conductivity of air according to the aforementioned standard varied depending on the exact dimensions of the cavities (Jóhannesson, 2006).

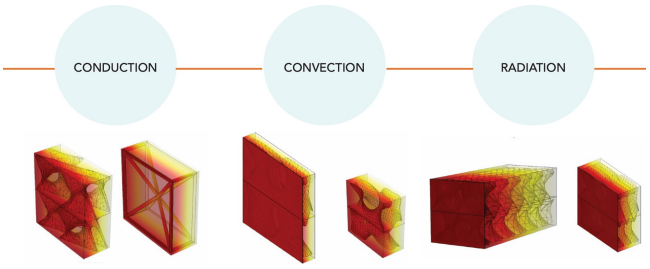

Figure 8: Varying parameters for heat transfer simulations in COMSOL Multiphysics

The simulation results are compared to those of the physical tests in Figure 9. A difference of 10% and 22% is found for the Gyroid and Diamond geometry respectively. This difference is small enough to consider the COMSOL model as a reliable one. For the Schwartz's P geometry, however, this difference increases to 40%. This could be explained by the fact that, contrary to the other two, this geometry was printed with a smaller shell thickness (1 mm instead of 2 mm) as part of the exploration of the manufacturing process. The resulting thermal conductivity from the physical tests would be higher in case the sample was

printed with a thicker shell, thus better aligning with the simulations results. Overall, the results of the simulations prove the reliability of the COMSOL model which is refined enough to approximate the physical heat transfer in cellular structures. The model also allows for a more accurate comparison of the different geometries, as possible inaccuracies in the model would affect the different geometries in the same way. On the contrary, inaccuracy of the measurements of the physical tests can differ from case to case in an unpredictable way.

Moreover, through the different steps of the simulation and testing process (Figure 10), some conclusions could be drawn regarding the thermal behaviour of cellular structures. When small air cavities are involved (up to 2 cm), heat transfer by convection is minimal and can be neglected. Both conduction and radiation contribute to the global heat transfer in cellular geometry, as we can see comparing the results of the simulations where only conduction is considered and those of the simulations where radiation is also considered (Figure 9). Overall, ratio of void-to-solid is the driving factor for thermal insulation. For this reason, lattices proved to be more efficient in thermal insulation.

According to the final simulation model, the average thermal conductivity of such geometries is 0.07 W/(m·K) which is lower than the average for shell geometries, 0,09 W/(m·K). From a geometrical point of view, the thermal resistance of lattices depends greatly on the porosity of the cell structure. The influence of porosity is less predictable in shell structures, where Schwartz's P geometry resulted to have higher thermal conductivity, in spite of its low relative density. In general, differences in results between the geometries are not very significant. Therefore, the choice of the best geometry to be explored in the façade panel design was done considering manufacturing aspects as well.

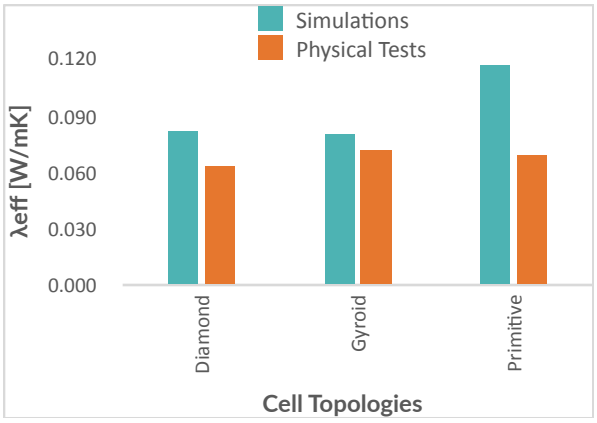

Figure 9: Comparison of simulations and physical tests results

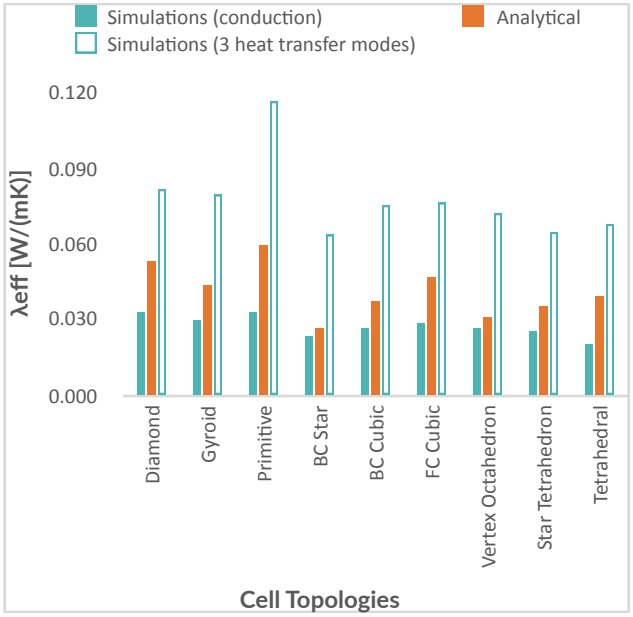

Figure 10: Comparison of results from simulations, analytical models and physical tests for different cell topologies

4. DIGITAL WORKFLOW

4.1. From simulations to performance-driven design

The study of heat transfer in cellular geometries is a complex one, consisting of radiation, convection and conduction. Analytical models are not able to account for convective and radiative heat transfer while finite element analysis is a powerful tool to estimate the thermal insulation property of cellular geometries. However, the use of a stand-alone software, outside the parametric environment of Rhino-grasshopper, resulted in the impossibility of integrating the results directly in the design process. To overcome this, the results of the software simulations and analytical models were compared and an analytical expression was proposed to retrieve an effective thermal conductivity for cellular structures. In particular, two different expressions are proposed for lattice and shell topologies respectively. These expressions are derived from the analytical models presented in Section 3.1 and are adjusted in order to account for radiative and convective heat transfer. This is done following the methodology of NEN-EN-ISO 6946, which consists in assigning a new thermal conductivity value to air. In particular, for lattice structures the model proposed by Ashby (2006) is used, which assumes that, in such geometries, 1/3 of the struts of the cellular structure lie parallel to one Cartesian axis. The expression, including the adjusted thermal conductivity value for air (λg), is:

$$\lambda_{cell} = \frac{2}{3}\left(\frac{\rho_{cell}}{\rho_s}\right) \bullet \lambda_s + \lambda_g$$

where:

- λs is the thermal conductivity of the bulk material [W/mK];

- λg is the adjusted thermal conductivity of air [W/mK]; - Vs is the volume of the bulk material [m^3];

- Vg is the volume of air [m^3];

For shell topologies, the model developed by Leach (1999) is used instead, which unifies the results of a number of approaches to calculate the conductivity of cellular structures. The expression, including the adjusted thermal conductivity value for air (λg), is:

$$\lambda_{cell} = \frac{1}{3}\left(\frac{\rho_{cell}}{\rho_s}\right) \bullet \lambda_s + \left[1 - \left(\frac{\rho_{cell}}{\rho_s}\right)\right]\lambda_g$$

where:

- λs is the thermal conductivity of the bulk material [W/mK];

- λg is the adjusted thermal conductivity of air [W/mK];

- ρs is the density of the bulk material [kg/m3];

- ρcell is the density of air [kg/m3];

The two expressions have been compared to the results of the software simulations and proved to be relatively accurate. In particular, as presented in Figure 11, for lattice topologies a mean approximation error of 10% was found while for shell topologies this accounted for 16%. By looking at the results in Figure 12, it can be noticed that the analytical results do not fluctuate much, giving very similar results for different topologies.

Another approach to retrieve an appropriate analytical expression for thermal conductivity is regression analysis. In particular, the relationship between effective thermal conductivity and cell porosity was estimated by the linear function:

$$y = -0.1347x + 0.1888$$

where:

- x is the porosity of the cell topology;
- the two numeric parameters represent the thermal properties of the solid and gas components.

As can be observed in Figure 11, this relation is accurate for all cell topologies except for the Schwartz's P geometry. A possible explanation for this is the fact that this particular shell topology is the only one featuring closed air bubbles, which may require further refinement of the model created in COMSOL Multiphysics. For the same reason, a considerable discrepancy between the results of the physical test (0,069 W/mK) and those of the simulations (0,116 W/mK) was found for the same cell topology.

Nevertheless, the two analytical expressions described above were found to be useful and accurate enough to be integrated and used within the digital workflow as a preliminary assessment tool for thermal performance. Figure 12 shows how the two expression have been integrated in the workflow. The user is required to input the material and geometrical properties and of the cellular structure (cell and cavity sizes), while relative density and porosity of the geometry come as output of the geometry generation part.

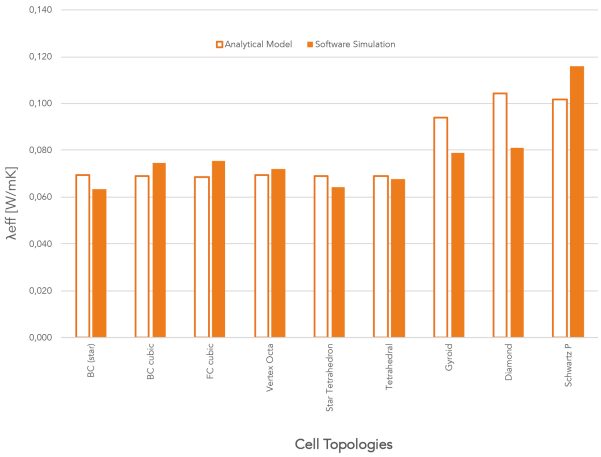

Figure 11: Comparison of simulations and physical tests results

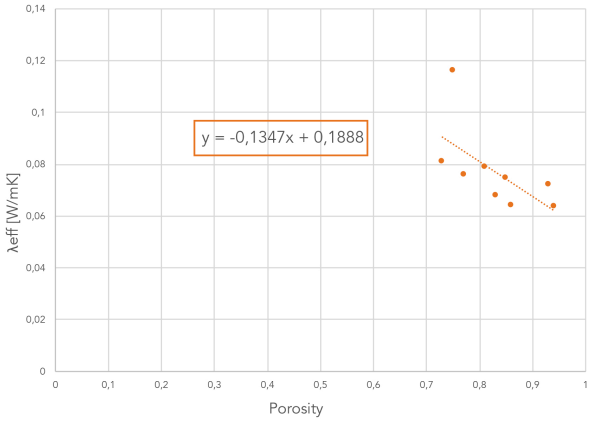

Figure 12: Comparison of simulations and physical tests results

4.2. Design work-flow

As outcome of this study a digital work-flow was defined for designing façade elements with complex geometries for thermal and structural performance. This can be used as a design tool through which the form of envelope components can be generated, according to loads acting on the façade and desired cell geometry. The geometry generated in the parametric model was analysed with FEA using a stand-alone software, COMSOL Multi-physics. In the last phase of the study, the results of the simulations in COMSOL were analysed and compared to the analytical models in order to find a simple analytical expression for the calculation of effective thermal conductivity which could be integrated within the parametric model. The same model was also used to generate sample geometries for additive manufacturing which were then tested for the thermal performance. At the cell scale, the script integrates procedures for generation and performance assessment of both shell and lattice geometries. At the component scale,

for ease of use in the design process, the script is designed specifically for shell geometries to be produced with FDM. However, this could be adapted to lattice geometries with minimal changes in the geometry morphing phase.

5. FAÇADE COMPONENT

The digital workflow was used to design a façade element of 3 x 1.5, in which the chosen cellular geometry is morphed to provide additional stiffness for the most stressed parts of the panel, thus enhancing its structural performance. In the less stressed areas, porosity increases improving thermal insulation. The geometry varies also within the panel thickness according to address the required performance using the same material (Figure 13). According to thermal analysis performed on the element, the component is able to comply with the current regulations regarding maximum deflection and Rc-value, making this a promising direction for further development of a marketable façade component.

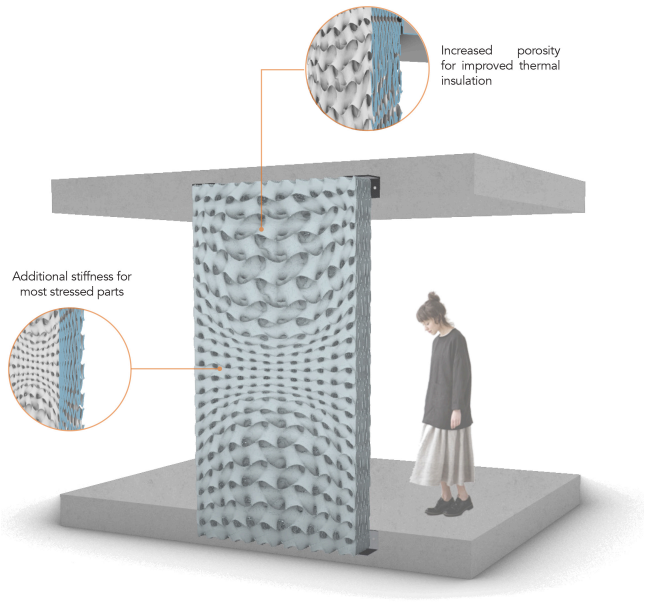

Figure 13: The AM envelope: results of the performance-driven design

5.1. Refinement of cell size

In order to optimise the overall design, the size of each cellular structure was increased to 25 x 25 x 3.4 mm, achieving a more porous yet stiff geometry and, therefore, a lower weight. The relation between cell size and relative density is shown in Figure 14 and depends on the implicit surface equation defined for the gyroid cell:

$$cos(x) \bullet sin(y)+cos(y) \bullet sin(z)+cos(z) \bullet sin(x) = 0$$

Increasing the cell dimension reduces the number of cells needed to fill the panel volume. Moreover, since porosity slightly increases along with the cell size, the weight of the panel can be reduced by more than 8%, reaching 101 kg. Increasing the cell size is also beneficial from a production point of view as printing time is decreased. Considering the thermal performance, simulations showed that increasing the cell size is beneficial as the relative density decreases. In fact, the thermal performance of the panel benefits from the lower thermal conductivity of air.

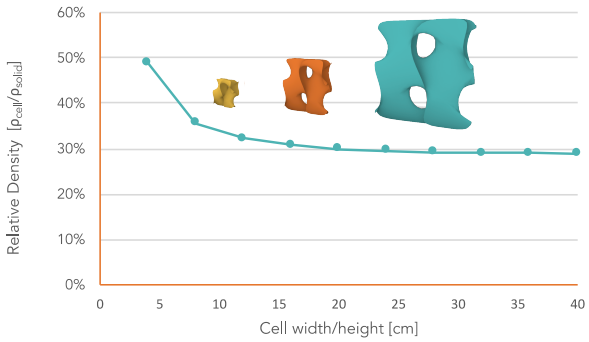

Figure 14: Relation between cell size and porosity in Gyroid cells

To verify the assumption stated above, new simulations were carried out on the bigger cell size geometry in COMSOL. For the simulation, the same set-up described in Section 3.3 was used. An effective thermal conductivity for air was assigned to the material to account for radiative and convective heat transfer, according to NEN-EN-ISO 6946. As expected, the thermal conductivity of the sample slightly decreases, reaching 0.065 W/mK. In order to achieve the prescribed Rc-value of 4.5 m^2K/W the façade panel is required a thickness of 29 cm.

6. CONCLUSIONS

This study aimed at investigating the thermal performance of cellular structures to be implemented into a multi-functional mono-material façade panel produced by additive manufacturing. The research focused on exploring the relation between geometry and performance at different design scales, making use of digital tools, prototyping and physical testing to design non-standard spatially varying geometries. According to the results, a methodology was proposed and embedded into a digital design workflow in Rhino-Grasshopper through which the panel geometry can be generated.

The results of the study showed that cellular geometries can be designed to achieve low thermal conductivity values by controlling the surface-to-volume ratio. Porosity is beneficial for decreasing thermal conductivity. However, heat transfer in cellular geometries also depends on convection and radiation. To minimise convection, air cavities should be kept within small widths and, therefore, elongated cells with small dimension in the direction of heat transfer were designed. Radiation accounts for a large part of the global heat transfer and shell geometries benefit from the shielding properties of the surfaces composing the cell. To minimise material use and cost, research towards further improvement of the thermal insulation could be carried out. Polymers with extremely low thermal conductivity and emissivity could achieve lower thermal conductivity values. The thermal conductivity of the gaseous component could be decreased if air is substituted with a noble gas such as argon and krypton.

The feasibility of the fabrication with AM was demonstrated through different production tests and a 1:1 prototype (Figure 15). This was done using an industrial 3D printer, prototyped by Leapfrog, featuring a massive build volume (55 x 50 x 250 cm) and equipped with a 1.2 mm nozzle extruder fed with PETG filament. The nature of the geometry makes it self-supporting and stiff so that no infill or supporting material is needed. The designed geometry proved to be suitable for large scale additive manufacturing, encouraging application of such geometries to the design of insulating façade components. Improving production efficiency is still required to scale up from prototype to building component. Further research and investigation are needed to define the façade concept as a marketable envelope component. Fast-paced advancements in the field of polymer large scale additive manufacturing are promoting novel applications for the building industry. The optimisation of production processes and tools are expected to lead to more competitive production costs in the short term (Dimensional Research, 2020). Moreover, material costs are also expected to decrease as more options enter the market.

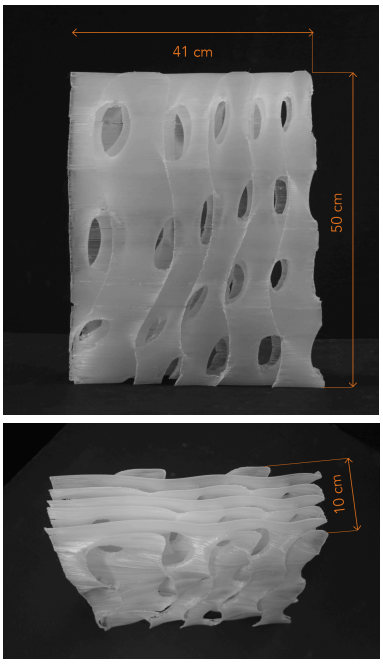

Figure 15: 1:1 scale prototype produced with FDM using PETG to test the feasibility of production with AM

7. ACKNOWLEDGEMENTS

The authors would like to acknowledge Ir. Paul de Ruiter (TU Delft – Architecture + Technology Department – Chair of Design Informatics), for his contributions in the prototyping phase, MSc(hons) Shibo Ren (ARUP Amsterdam), for his collaboration in the development of the computational workflow, and TOI LAMA Lab for Additive Manufacturing in Architecture.

8. REFERENCES

1. Ashby, M. F. *The properties of foams and lattices.* Philosophical Transactions of the Royal Society A: Mathematical, Physical and Engineering Sciences, 364 (2006), 15-30.
2. Dimensional Research. (2020). *Trends in 3D printing at scale:a survey of 3D printing stakeholders in production manufacturing* [Data set]. Retrieved from: https://cdn2.hubspot.net/hubfs/5442420/Content/Trends-in-3D-Printing-at-Scale.pdf
3. Gao, W., Zhang Y., Ramanujan D., Ramani K., Chen Y., Williams C. B., Wang C. C.L., Shin Y. C., Zhang S. & Zavattieri P. D. *The status, challenges, and future of additive manufacturing in engineering.* Computer-Aided Design, 69 (2015), 65-89.
4. Gooskens, G. 2016. *Printing properties: the potential of functionally graded cellular solids in the building envelope by integration of structural and thermal performance using the capabilities of additive manufacturing.* Repository Delft University of Technology (2016).
5. Hegman, N., Babscan, N. *Specific Feature of Thermal and Electrical Transport in Cellular Media* (2018).
6. Jóhannesson, G. Lectures on Building Physics: heat and moisture transfer. *Lecture notes, Building Physics AF1402.* KTH Royal Institute of Technology (2006).
7. Leach, A. G. Thermal conductivity of foams. I. *Models for heat conduction.* Journal of Physics D: Applied Physics. doi: 26. 733. 10.1088/0022-3727/26/5/003. (1999).
8. Meng, X., Gao, Y., Wang, Y.,Yan, B., Zhang, W. & Long, E. *Feasibility experiment on the simple hot box-heat flow meter method and the optimization based on simulation reproduction.* Applied Thermal Engineering, 48-56 (2015).
9. Nederlands Normalisatie Instituut. *Building components and building elements - Thermal resistance and thermal transmittance - Calculation method.* 2008 NEN-EN-ISO 6946. (2008).
10. Ngo, T. D., Kashani, A., Imbalzano, G., Nguyen, K. T.Q. & Hui, D. 2018. *Additive manufacturing (3D printing): A review of materials, methods, applications and challenges.* Composites Part B: Engineering. 143, 172-196..
11. Sarakinioti, M. V., Turrin, M., Konstantinou, T., Tenpierik, M. and Knaack, U. *Developing an integrated 3D-printed façade with complex geometries for active temperature control.* Materials Today Communications (15): 275-279 (2018).
12. Wu, P., Wang, J. & Wang, X. *A critical review of the use of 3-D printing in the construction industry.* Automation in Construction, 68, 21-31 (2016).
13. *About the 3D printed Canal House: Construction Technique.* Accessed September 15th 2018. https://3dprintcanalhouse.com/